Conclusions

The prominent 8983-eV feature present on the absorption edge of Cu(I) complexes is sensitive not only to overall coordination number (as documented previously by Kau and co-workers[26]) but also to the details of the symmetry of the complex. Thus, in all the complexes studied a correlation was found between the intensity of this feature and the degree of distortion of the complex from two- or three-coordinate planar geometry toward tetrahedral.

These correlations have been applied to predict the geometry of the Cu(I) sites of SOD, DBH, and deoxy-Hc. Assignment of Cu(I)–SOD as a planar (or closely planar) three-coordinate center is possible. In the latter two cases the presence of more than one structural type of Cu(I) complicates the analysis, but comparison of the edge profile of deoxy-Hc with those of the model systems suggests distorted three- or four-coordination and hence the possible presence of an endogenous hydroxyl bridge.

The technique is particularly valuable in the study of ligand binding to Cu(I) centers in proteins. Here, comparative changes in absorption edge features allow ligand binding to be detected and any consequent changes in coordination geometry to be predicted. Using the latter approach, we have demonstrated the existence of a CO complex of DBH. In the case of *B. canaliculatum* deoxy-Hc, changes in the absorption edge upon CO binding to a single Cu atom[43] are consistent with trigonal-pyramidal or pseudotetrahedral geometry at each copper center of the dinuclear unit. The data indicate that each Cu center in Hc–CO is three- or four-coordinate and argue against previous proposals of two- plus four-coordination in Hc–CO.

Acknowledgment. We thank the Daresbury Laboratory for provision of beam time, computational facilities, and other necessary equipment for this study. Financial support is gratefully acknowledged from the SERC to N.J.B., NIH to K.D.K., and ZWO to J.R. We also thank the NATO Scientific Affairs Bureau for the award of a travel grant (RG.82/0139) to N.J.B. and K.D.K.

Supplementary Material Available: Listings of bond lengths, bond angles, anisotropic temperature factors, and hydrogen coordinates and temperature factors for complex **3**-$(PF_6)_2$·CH_2Cl_2 (Tables 4–7) (10 pages); listings of observed and calculated structure factors for **3**-$(PF_6)_2$·CH_2Cl_2 (Table 8) (38 pages).

Contribution from the Department of Chemistry, University of Georgia, Athens, Georgia 30602, and Department of Physics, Emory University, Atlanta, Georgia 30322

Observation of $S = 2$ EPR Signals from Ferrous Iron–Thiolate Complexes. Relevance to Rubredoxin-Type Sites in Proteins

Mark T. Werth,[†] Donald M. Kurtz, Jr.,*[,†] Barry D. Howes,[‡] and Boi Hanh Huynh[‡]

Received September 15, 1988

In frozen solution the pseudotetrahedral ferrous iron–thiolate complexes with 2-mercaptoethanol, dithiothreitol, and glutathione (γ-glutamylcysteinylglycine) exhibit a low-field ($g \sim 10$) EPR signal below 30 K. This signal is ascribed to a transition within the $|\pm 2\rangle$ doublet of the $S = 2$ spin state, and these complexes appear to be the first examples of pseudotetrahedral ferrous complexes that give rise to such a signal. A detailed study was undertaken to ascertain the origin of this signal in the case of the complex with 2-mercaptoethanol. $Ba[Fe(SCH_2CH_2OH)_4]$ was prepared and shown to contain an FeS_4 site of approximate tetrahedral symmetry by X-ray crystallography. For $[Fe(SCH_2CH_2OH)_4]^{2-}$ in water, the 1–/2– midpoint reduction potential (–0.35 V vs SCE) and ^1H NMR (δ(Fe–SCH_2CH$_2$OH) 203 ppm at 25 °C) and ^{57}Fe Mössbauer ($\Delta E_Q = 3.48 \pm 0.03$ mm/s, $\delta = 0.73 \pm 0.02$ mm/s at 4.2 K) spectra show that this complex, and essentially only this complex, survives in solution, when the mole ratio of thiolate to iron is 4 or greater. Mössbauer spectra obtained in applied fields up to 7 T reveal at least two species in frozen aqueous solutions of $[Fe(SCH_2CH_2OH)_4]^{2-}$. Spectral simulations show that the major (75%) and minor (25%) species have spin Hamiltonian parameters strongly resembling those of reduced rubredoxin and reduced desulforedoxin, respectively. The minor species has values of zero-field splitting parameters ($D = -5.0 \pm 2.0$ cm^{-1}, $E/D = 0.17 \pm 0.05$) that are consistent with observation of an $S = 2$ EPR signal at low field. The slightly larger values of these parameters for reduced desulforedoxin preclude the observation of an $S = 2$ EPR signal from this protein. The two species of $[Fe(SCH_2CH_2OH)_4]^{2-}$ in solution are ascribed to different sets of S–Fe–S angles. Since variations in these angles are expected to have relatively low energy barriers, observation of an $S = 2$ EPR signal from biological Fe(Cys-S)$_4$ sites is likely to be strongly dependent on the protein matrix.

As part of a search for new spectroscopic probes of high-spin ferrous centers in proteins, we have examined the simplest such prototype for iron–sulfur proteins, namely, the pseudotetrahedral Fe(Cys-S)$_4$ site in reduced rubredoxin (Cys-S = cysteine thiolate). We have recently added ^1H NMR to the list of spectroscopies that can elicit characteristic signals from the ferrous Fe(Cys-S)$_4$ site in rubredoxin.[1] Judging from a number of recent reports,[2-5] EPR signals arising from integer spin states represent an increasingly important electronic probe of iron sites in proteins. We now report that the $S = 2$ state of ferrous $Fe(SR)_4$ complexes can exhibit a characteristic EPR signal. We also delineate some structural and spectroscopic parameters that favor observation of such a signal.

Experimental Section

All manipulations were carried out at room temperature under an Ar atmosphere in either Schlenk-type glassware or septum-capped vials attached to a vacuum manifold. Solutions were added and transferred via steel tubing or gastight syringes. The thiols used for this study, 2-mercaptoethanol, dithiothreitol, glutathione, and lipoic acid, were obtained commercially and used without further purification. D,L-Dihydrolipoate was prepared from the oxidized compound as previously described.[6] The following general procedure was used to prepare ferrous $Fe(SR)_4$ complexes in situ. The thiol was dissolved in the desired solvent (either water or DMSO) with sufficient LiOH to deprotonate thiol groups plus any carboxylate groups. Iron was then added as solid $FeCl_2$ or $Fe(SO_4)\cdot 7H_2O$. A thiolate/iron mol ratio ≥ 4 was maintained in all solutions. This procedure was previously shown to generate stable solutions of the ferrous $Fe(SR)_4$ complexes in water.[1] Specific reagent concentrations are given in the figure legends. Solutions for electrochemistry were ~4 mM in iron and ~100 mM in total thiol. These

[†] University of Georgia.
[‡] Emory University.

(1) Werth, M. T.; Kurtz, D. M., Jr.; Moura, I.; LeGall, J. *J. Am. Chem. Soc.* **1987**, *109*, 273–275.
(2) Hendrich, M. P.; Debrunner, P. G. *J. Magn. Reson.* **1988**, *78*, 133–141.
(3) Reem, R. C.; Solomon, E. I. *J. Am. Chem. Soc.* **1987**, *109*, 1216–1226.
(4) Hagen, W. R.; Dunham, W. R.; Johnson, M. K.; Fee, J. A. *Biochim. Biophys. Acta* **1985**, *828*, 369–374.
(5) Hagen, W. R. *Biochim. Biophys. Acta* **1982**, *708*, 82–98.
(6) Bonomi, F.; Werth, M. T.; Kurtz, D. M., Jr. *Inorg. Chem.* **1985**, *24*, 4331–4335.

0020-1669/89/1328-1357$01.50/0

latter solutions typically contained 100 mM Et_4NBF_4 as supporting electrolyte.

Ba[Fe(SCH$_2$CH$_2$OH)$_4$]. To 50 mL of water were sequentially added 6.42 g (20.4 mmol) of $Ba(OH)_2 \cdot 8H_2O$, 7.1 mL (100 mmol) of 2-mercaptoethanol, and 2.79 g of (10.0 mmol) $Fe(SO_4) \cdot 7H_2O$. The heterogeneous reaction mixture was stirred for 75 min, after which a white solid (presumably $BaSO_4$) settled from a dark yellow solution. The top 20–30 mL of solution was transferred to another flask. Solvent was then removed from this solution by evacuation until a thick oil was obtained. Slow addition of roughly 8 volumes of acetone with stirring produced the sudden precipitation of off-white crystals. Separation of the crystals from solvent, washing with methanol, and thorough drying under dynamic vacuum resulted in a 54% yield of analytically pure Ba[Fe(SCH$_2$CH$_2$OH)$_4$]. Anal. Calcd for $C_8H_{20}O_4BaFeS_4$: C, 19.15; H, 4.02; Ba, 27.38; Fe, 11.13; S, 25.56. Found: C, 19.28; H, 4.12; Ba, 27.60; Fe, 11.11; S, 25.94. ^{1}H NMR (DMSO-d_6, δ in ppm): 211, ~12, 6.2. Absorption spectrum (DMSO; λ_{max}, nm (ϵ_M)): 316 (5800), 340 sh (3200). A single-crystal X-ray diffraction study of this compound was carried out by Elizabeth Holt at Oklahoma State University.[7]

Physical Measurements. ^{1}H NMR spectra were obtained at ~23 °C on a Bruker Model AM-250 spectrometer. Shifts downfield of the Me_4Si reference are designated as positive. Cyclic voltammetry was performed on Ar-purged solutions with a Bioanalytical Systems Model 100 electrochemical analyzer equipped with a glassy-carbon working electrode and an Ag/AgCl reference electrode. Scan rates in the range 10–250 mV/s were used. Experimentally obtained values of $E_{1/2}$ were corrected to the SCE reference electrode by subtraction of 0.01 V. First-derivative EPR spectra were recorded on an IBM Model ER-220D spectrometer equipped with an Oxford Instruments Model ESR-9 cryostat. Samples were placed in 4-mm-o.d. quartz tubes under Ar and frozen in liquid N_2.

Solutions of $[Fe(SCH_2CH_2OH)_4]^{2-}$ for Mössbauer spectroscopy were prepared according to the general procedure in aqueous solution using the natural isotopic abundance of ^{57}Fe (2.2%). Approximately 0.3 mL of solution was transferred to a nylon cylindrical Mössbauer sample cup that had been chilled to liquid N_2 temperature. Samples were thereafter stored frozen at liquid N_2 temperature. ^{57}Fe Mössbauer spectra were recorded on two spectrometers, one for weak-field and one for strong-field measurements. Both spectrometers used a constant acceleration and standard transmission arrangement. The weak-field spectrometer was equipped with a Ranger VT-700 velocity transducer and a top-loading Janis 8DT SuperVaritemp cryostat. The strong-field spectrometer was equipped with a top-loading Janis 12 CNDT/SC SuperVaritemp cryostat complete with an American Magnetics 8-T superconducting magnet and a home-built Doppler velocity transducer. The γ-ray source was purchased from New England Nuclear and was made by electrodeposition of 50-mCi ^{57}Co onto a 0.006 mm thick rhodium foil. Absorber temperatures were controlled by a Lake Shore 520 cryogenic temperature controller. The velocity scale was calibrated by using the room-temperature Mössbauer spectrum of a metallic iron foil absorber. Zero velocity was taken to be the centroid of the iron-foil spectrum.

Results

A quasi-reversible wave (ΔE_p = 75 mV, i_a/i_c = 1.04) was observed for Ba[Fe(SCH$_2$CH$_2$OH)$_4$] in DMSO by cyclic voltammetry yielding a midpoint reduction potential, $E_{1/2}$ = −0.81 V vs SCE. This wave, which requires excess thiol for quasi-reversibility, is reasonably assigned to the $[Fe(SCH_2CH_2OH)_4]^{1-/2-}$ couple. The value of $E_{1/2}$ is more positive than the −1.08 V measured for $[Fe(SCH_2CH_3)_4]^{1-/2-}$ (in CH_3CN);[9] the more positive value can be rationalized as due predominantly to the electron-withdrawing hydroxyl substituent.[10,11] A single-crystal X-ray diffraction study confirmed the pseudotetrahedral FeS_4 structure in Ba[Fe(SCH$_2$CH$_2$OH)$_4$].[7]

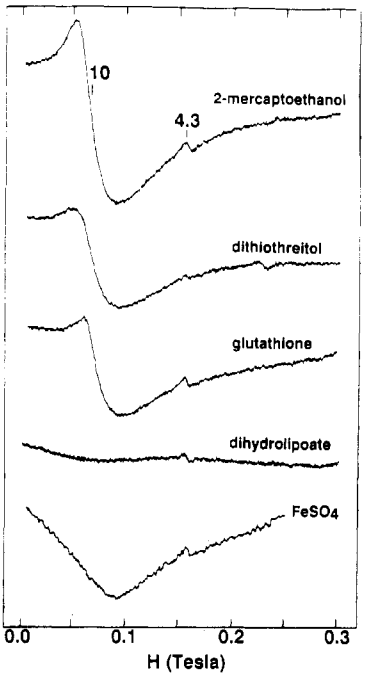

Figure 1. EPR spectra of ferrous $Fe(SR)_4$ complexes of, from top to bottom, 2-mercaptoethanol, dithiothreitol, glutathione, and D,L-dihydrolipoate. Solutions were prepared in water as described in the Experimental Section and in ref 1. The solutions were 40 mM in thiol (20 mM in dithiol) and LiOH and 10 mM in $FeCl_2$. The lowest spectrum is of an ~11 mM aqueous solution of $FeSO_4$. EPR conditions: T, 5–7 K; frequency, 9.41 GHz; power, 0.2 mW; modulation, 16 G at 100 kHz; time constant, 0.16 s. Positions of g = 10 and 4.3 are indicated on the top spectrum. The g = 4.3 feature is due to a small amount of rhombic high-spin Fe^{3+} impurity.

Due to the high-absorption cross section of barium for γ-rays, Ba[Fe(SCH$_2$CH$_2$OH)$_4$] could not be examined by Mössbauer spectroscopy. The powder EPR spectrum of this solid shows only a broad feature extending from $g_{max} \sim 9$ to $g_{min} \sim 3$, which we attribute to an integer spin state. This EPR spectrum is presumably complicated by magnetic dipolar interactions among neighboring iron atoms, which are <7 Å apart in the crystal. In order to circumvent these difficulties, concentrated aqueous solutions of $[Fe(SCH_2CH_2OH)_4]^{2-}$ were prepared as described in the Experimental Section for detailed examinations by Mössbauer and EPR spectroscopies. These solutions exhibited absorption (λ_{max} 309 nm) and ^{1}H NMR (δ(Fe–SCH_2CH$_2$OH) 203 ppm at 25 °C in D_2O) spectra[1] very similar to those of Ba[Fe(SCH$_2$CH$_2$OH)$_4$] in DMSO. The ^{1}H NMR spectra revealed no resonances attributable to ferrous iron–thiolate clusters, such as $[Fe_2(SR)_6]^{2-}$ or $[Fe_4(SR)_{10}]^{2-}$, that have pseudotetrahedral coordination geometries.[12,13] Furthermore, the reduced paramagnetism of these clusters relative to that of the mononuclear complexes is indicative of antiferromagnetic coupling within the clusters. No such coupling was evident in the magnetic Mössbauer spectra obtained in the present work (vide infra). Aqueous solutions of $[Fe(SCH_2CH_2OH)_4]^{2-}$ reproducibly exhibited quasi-reversible waves (e.g., ΔE_p = 103 mV, i_a/i_c = 1.04) yielding $E_{1/2}$ = −0.35 V vs SCE. The increase of ~0.46 V in the value of the midpoint reduction potential on changing the solvent from DMSO to water is similar in magnitude to that observed for the cubane

(7) General procedures for collection and reduction of the X-ray data and solution and refinement of the structure are given elsewhere.[8] Crystal data: Ba[Fe(SCH$_2$CH$_2$OH)$_4$], mol wt = 501.7, tetragonal $P\bar{4}$, Z = 1, d_{calcd} = 1.945 g/cm^{-3}, $a = b$ = 6.900 (4) Å, c = 8.995 (5) Å, $\alpha = \beta = \gamma$ = 90.00°, $F(000)$ = 246, μ = 36.02 cm^{-1} for Mo Kα radiation (λ = 0.71069 Å, graphite monochromated), number of measured reflections = 305, number of observed reflections = 299, $R = \sum||F_o| - |F_c||/\sum|F_o|$ = 9.7%. While the diffraction data were of sufficient quality to establish the positions of the Ba, Fe, and S atoms, disorder of the hydroxyethyl groups is clearly evident in the bond distances derived for these atoms from the positions of the final refinement and in the magnitudes of the anisotropic thermal parameters for these atoms (deposited as supplementary material). The FeS_4 site is centered on the crystallographic $\bar{4}$ symmetry element and, therefore, has D_{2d} point group symmetry. The Fe–S bond length is 2.30 (2) Å. The S–Fe–S bond angles are 108.3 (6) and 111.9 (6)°.

(8) King, R. B.; Wu, F.-J.; Holt, E. M. *J. Am. Chem. Soc.* **1987**, *109*, 7764–7775.

(9) Hagen, K. S.; Holm, R. H. *J. Am. Chem. Soc.* **1982**, *104*, 5496–5497.

(10) Millar, M.; Lee, J. F.; Koch, S. A.; Fikar, R. F. *Inorg. Chem.* **1982**, *21*, 4105–4106.

(11) Ueyama, N.; Nakata, M.; Fuji, M.; Terakawa, T.; Nakamura, A. *Inorg. Chem.* **1985**, *24*, 2190–2196.

(12) Hagen, K. S.; Holm, R. H. *Inorg. Chem.* **1984**, *23*, 418–427.

(13) $[Fe_4(SCH_2CH_2OH)_{10}]^{2-}$ was evident in ^{1}H NMR spectra (δ(Fe–SCH_2) ~140 (b) and ~110 ppm (t)) only when the mole ratio of thiolate/ferrous iron was <4.[14]

(14) Werth, M. T. Ph.D. Thesis, Iowa State University, 1989.

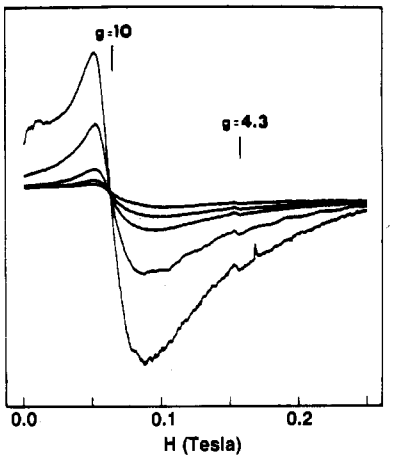

Figure 2. Temperature dependence of the low-field EPR signal from $[Fe(SCH_2CH_2OH)_4]^{2-}$. The solution was prepared in water as described in the Experimental Section. Final reagent concentrations were 470 mM LiOH, 600 mM 2-mercaptoethanol, and 60 mM $Fe(SO_4)\cdot 7H_2O$. EPR conditions are the same as for Figure 1. Sample temperatures in order of decreasing signal intensity were 4, 8, 13, 18, and 28 K.

cluster, $[Fe_4S_4(SCH_2CH_2OH)_4]^{1-/2-}$.[15]

The preceding results collectively establish that $[Fe(SCH_2CH_2OH)_4]^{2-}$ is the species observed by Mössbauer and EPR spectroscopies in this study. Absorption and ^1H NMR spectra[1] strongly suggest analogous formulations for the ferrous complexes of glutathione, dithiothreitol, and D,L-dihydrolipoate prepared in this work. The ^1H NMR spectra of the latter two complexes are consistent with a bis S,S′-bidentate chelate formulation.

Figure 1 shows EPR spectra of aqueous solutions of the ferrous $Fe(SR)_4$ complexes with various thiols. For $[Fe(SCH_2CH_2OH)_4]^{2-}$ the $S = 2$ signal is centered at $g \sim 10$ with maxima and minima at $g \sim 12.7$ and $g \sim 7.5$, respectively. The line shapes and g values for the complexes with dithiothreitol and glutathione are very similar to those of $[Fe(SCH_2CH_2OH)_4]^{2-}$, whereas the D,L-dihydrolipoate complex shows no EPR signal. Figure 1 also shows for comparison the low-field EPR signal of an aqueous solution of ferrous sulfate. This comparison shows that the ferrous $Fe(SR)_4$ complexes exhibit a low-field signal with a much different line shape than that of $Fe^{2+}(aq)$. Figure 2 shows that the EPR signal of $[Fe(SCH_2CH_2OH)_4]^{2-}$ decreases in intensity with increasing temperature. The signal disappears completely at ~30 K. A very similar temperature dependence was found for the ferrous $Fe(SR)_4$ complex of dithiothreitol.[14] Between 5 and 7 K these signals continue to increase in intensity up to a microwave power of at least 20 mW. Due to variations in spin-state populations and transition probabilities among various complexes, no reliable standard solutions are available for quantitation of spin concentrations for these $S = 2$ signals.

Mössbauer spectra of frozen solutions of $[Fe(SCH_2CH_2OH)_4]^{2-}$ were recorded at 4.2 K over a wide range of applied magnetic fields (0–7 T). Additional spectra were recorded at higher temperatures (90, 130, and 170 K) with a fixed applied field of 7 T. Figure 3 shows a 4.2 K spectrum recorded in the absence of a magnetic field. A single quadrupole doublet was observed. The Mössbauer parameters ($\Delta E_Q = 3.48 \pm 0.03$ mm/s, $\delta = 0.73 \pm 0.02$ mm/s)[16] obtained by least-squares fitting of the data are typical of high-spin ferrous compounds ($S = 2$) with tetrahedral sulfur coordination.[17,18] These parameters are also very similar to those found for rubredoxins from *Clostridium pasteurianum* and *Desulfovibrio vulgaris* and are identical with those of desulforedoxin from *Desulfovibrio gigas*.[19,20] As for these proteins, the quadrupole splitting of $[Fe(SCH_2CH_2OH)_4]^{2-}$ was found to be temperature independent, and at 170 K, ΔE_Q remained 3.48 mm/s. This observation indicates that the first-excited orbital state must be well separated from the ground spin quintet, which greatly simplified our data analysis.

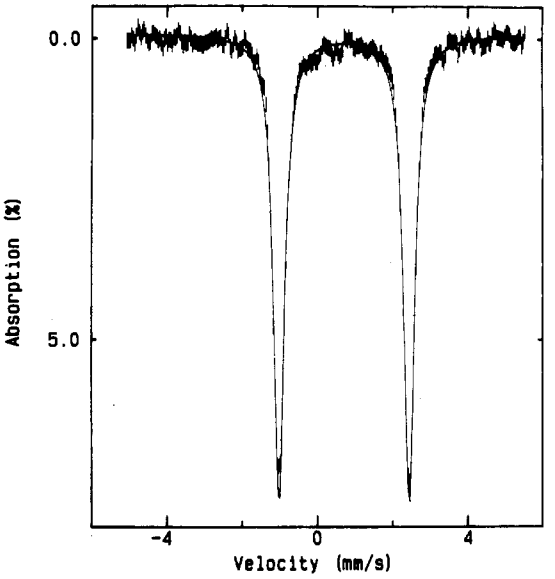

Figure 3. Mössbauer spectrum of a frozen aqueous solution of $[Fe(SCH_2CH_2OH)_4]^{2-}$. The sample contained 467 mM LiOH, 595 mM 2-mercaptoethanol, and 60 mM ferrous sulfate. The spectrum was recorded at 4.2 K in zero field. The solid curve represents the least-squares fit from which the values of the isomer shift and quadrupole splittings listed in Table I were obtained.

For high-spin ferrous complexes, the spin degeneracy of the ground quintet is generally lifted by the spin–orbit interaction and, in the absence of an applied field, the expectation values, $\langle \vec{S} \rangle$, of the five spin states are equal to zero. The zero-field Mössbauer spectrum is therefore a simple quadrupole doublet, as presented above. However, in the presence of a strong magnetic field, nonzero values of $\langle \vec{S} \rangle$ are induced, and the Mössbauer spectrum exhibits magnetic splitting governed by the induced internal field $\vec{H}_{int} = -\langle \vec{S} \rangle \cdot \vec{A}/g_n\beta_n$. Figure 4 shows 4.2 K spectra of $[Fe(SCH_2CH_2OH)_4]^{2-}$ recorded in parallel applied fields up to 7 T. At least two species, which have internal fields that display different saturation behavior, were observed in these spectra. The evidence of the presence of two species was most obvious in the 0.5- and 1-T spectra. The basic pattern of the 0.5-T spectrum (Figure 4A) can be viewed as a quadrupole doublet with its absorption lines split by a weak internal field (i.e., small $\langle \vec{S} \rangle$), resulting in the double-peak pattern observed for each absorption line. In addition to the magnetically split quadrupole doublet, a shoulder and peaks were observed at velocities of −3.2, +0.3, and +4.7 mm/s (marked by arrows in Figure 4), respectively, suggesting the presence of a minor species with a much larger $\vec{H}_{int}$. At 1 T, the $\vec{H}_{int}$ of the major species increased in magnitude, resulting in the larger splitting observed for each absorption line of the quadrupole doublet. The positions of the absorption lines of the minor species remained virtually unchanged. These observations indicated that the $\vec{H}_{int}$ of the minor species is readily saturated at an applied field of 0.5 T, while that of the major species remains unsaturated. Studies performed with stronger applied fields indicated that the $\vec{H}_{int}$ of the major species saturated at ~2 T. In spectra recorded with applied fields stronger than 2 T (see spectrum D of Figure 4), the two subspectral components

(15) Hill, C. L.; Renaud, J.; Holm, R. H.; Mortenson, L. E. *J. Am. Chem. Soc.* **1977**, *99*, 2549–2557.
(16) For both absorption lines, the full width at half-maximum was 0.35 mm/s, which compares reasonably well with those generally observed for proteins.
(17) Lane, R. W.; Ibers, J. A.; Frankel, R. B.; Papaefthymiou, G. C.; Holm, R. H. *J. Am. Chem. Soc.* **1977**, *99*, 84–98.
(18) Coucouvanis, D.; Swenson, A.; Baenziger, N. C.; Murphy, C.; Holah, D. G.; Sfarnas, N.; Simopoulos, A.; Kostikas, A. *J. Am. Chem. Soc.* **1981**, *103*, 3350–3362.
(19) Moura, I.; Huynh, B. H.; Hausinger, R. P.; Le Gall, J.; Xavier, A. V.; Münck, E. *J. Biol. Chem.* **1980**, *255*, 2493–2498.
(20) Huynh, B. H.; Kent, T. In *Advances in Mössbauer Spectroscopy*; Thosar, B. V., Iyengar, P. K., Eds.; Elsevier Publishing Co.: New York, 1983; Chapter 9, pp 490–560.

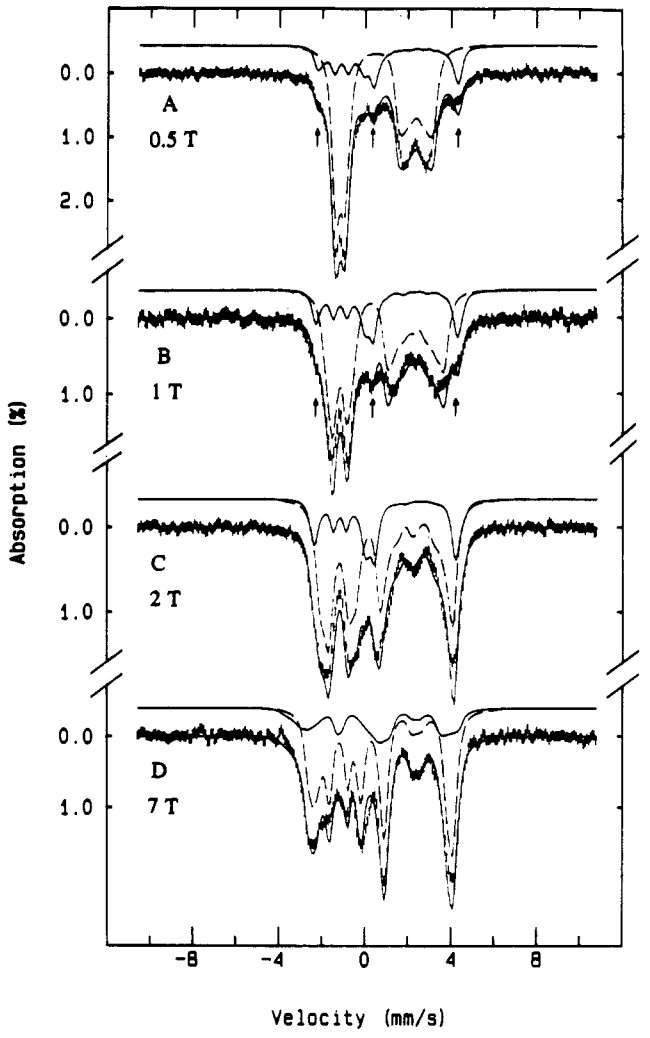

Figure 4. Mössbauer spectra of the solution of Figure 3 at 4.2 K and applied magnetic fields of indicated values. The magnetic fields are applied parallel to the γ-ray beam. The solid curves plotted over the data are theoretical simulations using the parameters listed in Table I. For the major and minor species, 75% and 25%, respectively, are assumed in the simulations. Theoretical spectra for the major (—) and minor (- - -) species are also shown.

corresponding to the two species were unresolved, suggesting that the saturated internal fields for both species are very similar.

The saturation behavior of $\vec{H}_{int}$ as a function of applied field is governed by the energy separation, Δ, between the two lowest spin states of the $S = 2$ quintet; the smaller the value of Δ, the faster $\vec{H}_{int}$ reaches its saturation value. The different saturation behavior observed for the two species implies that their energy level structures differ. To gain further information concerning the electronic structures of the two species, we analyzed the data using the following $S = 2$ spin Hamiltonian:

$$\hat{H} = D[S_z^2 - S(S+1)/3 + (E/D)(S_x^2 - S_y^2)] + \beta(\vec{S})\cdot\tilde{g}\cdot\vec{H} + \langle\vec{S}\rangle\cdot\tilde{A}\cdot\vec{I} + (eEQV_{zz}/4)[I_z^2 - I(I+1)/3 + (\eta/3)(I_x^2 - I_y^2)] - g_n\delta_n\vec{H} \quad (1)$$

where $\eta = (V_{xx} - V_{yy})/V_{zz}$. D and E, respectively, are the axial and rhombic zero-field splitting parameters. For $D > 0$

$$\Delta = D\{2[1 + 3(E/D)^2]^{1/2} - 1 - 3E/D\} \quad (2)$$

and for $D < 0$

$$\Delta = 2D\{1 - [1 + 3(E/D)^2]^{1/2}\} \quad (3)$$

From detailed spectral simulations[21] using eq 1 while keeping D in a reasonable range (1–10 cm^{-1}) and $E/D < {}^1/_3$ (the proper axis system), we found that $D > 0$ and $\Delta \sim 4$ cm^{-1} for the major species and $D < 0$ and $\Delta = 0.3$–0.5 cm^{-1} for the minor species. In these situations, the low-temperature Mössbauer spectra of the major species are sensitive to their hyperfine parameters along the y axis, while those of the minor species are sensitive to parameters along the z axis. Consequently, these parameters could be determined with accuracy. The remaining parameters were determined through a series of simulations and by visually comparing the simulated spectra with their experimental counterparts.[22] The parameters thus obtained are listed in Table I, and the theoretical simulations are plotted in Figure 4 as the solid curves. An assumption of 75% for the major species and 25% for the minor species yielded the best agreement between theory and experiment.

Table I. Spin Hamiltonian Parameters for the Major and Minor Species in the Mössbauer Spectra of $[Fe(SCH_2CH_2OH)_4]^{2-}$

	major species	minor species
D, cm^{-1}	8.0 ± 1.0	−5.0 ± 2.0
E/D	0.20 ± 0.02	0.17 ± 0.05
g_x[a]	2.11	2.08
g_y	2.19	2.02
g_z	2.20	2.00
$A_{xx}/g_n\beta_n$, T[b]	−15.0 ± 2.0	−20.0 ± 2.5
$A_{yy}/g_n\beta_n$, T	−8.5 ± 0.5	−25.0 ± 5.0
$A_{zz}/g_n\beta$n, T	−25.0 ± 5.0	−6.7 ± 0.3
ΔE_Q, mm/s	−3.48 ± 0.03	3.48 ± 0.03
η	0.75 ± 0.10	0.35 ± 0.10
δ, mm/s	0.73 ± 0.02	0.73 ± 0.02

[a] The electronic g values for the major and minor species were assumed to be the same as those obtained for rubredoxin and desulforedoxin, respectively (cf. ref 19 and 20). [b] The symbol β_n represents the nuclear magneton, and g_n has the values 0.1806 and −0.1033 for the ground and excited states of the ^{57}Fe nucleus.

Discussion

Low-field EPR signals from high-spin ferrous iron have been attributed to a transition within the $|\pm2\rangle$ doublet of the $S = 2$ spin state.[5] For $D < 0$ this doublet is lowest in energy, and in a zero field of rhombic symmetry, the energy separation, Δ, between the $|2^s\rangle$ and $|2^a\rangle$ levels (using the notation of Abragam and Bleaney)[24] is given by eq 3.[25] For an X-band EPR spectrometer, the energy quantum is $\simeq 0.3$ cm^{-1}. Since the applied magnetic field in the EPR experiment superimposes Zeeman splitting onto the zero-field splitting of the $|m_s = \pm2\rangle$ doublet, a requirement for observability of the $S = 2$ EPR signal is $\Delta \lesssim 0.3$ cm^{-1}. The Mössbauer parameters of Table I indicate that the minor species ($\sim$25% of total iron) in the aqueous solutions of $[Fe(SCH_2CH_2OH)_4]^{2-}$, having $D < 0$ and $\Delta = 0.3$–0.5 cm^{-1}, meets this requirement within experimental error. We, therefore, assign the corresponding EPR signals of Figures 1 and 2 to this minor species. Additional evidence for the correctness of this assignment comes from the *rapid* decrease in EPR signal intensity as the temperature is raised above 4 K. Such dependence indicates that this low-field signal arises from a ground-state doublet, as expected for $D < 0$. The major species observed by Mössbauer spectroscopy has $\Delta \sim 4$ cm^{-1}, which is much too large for occurrence of a low-field EPR resonance at X-band.

The spin Hamiltonian parameters of Table I for the major and minor species of $[Fe(SCH_2CH_2OH)_4]^{2-}$ in solution are similar to those of reduced rubredoxin and reduced desulforedoxin, respectively.[19,20] Therefore, on the basis of the preceding discussion, one does not expect reduced rubredoxin to exhibit a low-field EPR

(21) A line width of 0.35 mm/s and a slow electronic relaxation rate (<10^{-8} s) were used in these simulations.

(22) A detailed methodology for the data analysis of high-spin ferrous compounds is discussed in ref 23.

(23) Zimmerman, R.; Huynh, B. H.; Münck, E.; Lipscomb, J. D. *J. Chem. Phys.* **1978**, *69*, 5463–5467.
(24) Abragam, A.; Bleaney, B. *Electron Paramagnetic Resonance of Transition Ions*; Clarendon Press: Oxford, U.K., 1970; Chapter 3, pp 209–216.

(25) The equations for Δ given by Hagen[5] are approximations when $E/D \ll 1$.

transition. Although $D < 0$ for reduced desulforedoxin, the calculated value $\Delta = 0.6$ cm^{-1} [19] is too large for observation of an $S = 2$ EPR signal. We have verified that no such signal is observed from reduced desulforedoxin.[14] The possibility remains, however, that the similarities in spin Hamiltonian parameters of the major and minor species of $[Fe(SCH_2CH_2OH)_4]^{2-}$ to those of the two proteins reflect two energetic minima in the FeS_4 ligand field rather than coincidence. Such minima could occur as a result of Jahn-Teller effects.[17,18] The differing sets of spin Hamiltonian parameters for reduced rubredoxin and reduced desulforedoxin were originally interpreted as reflecting different orbital ground states: predominantly d_{z^2} for rubredoxin and predominantly $d_{x^2-y^2}$ for desulforedoxin.[19,20] These different ground states presumably reflect different FeS_4 stereochemistries. A more recent analysis[26] assumes D_2 symmetry for the FeS_4 site and uses a common set of ligand field energies for the two reduced proteins. The differing sets of spin Hamiltonian parameters, including the opposite signs of D, can be fit reasonably well by small variations in the degree of mixing the d_{z^2} and $d_{x^2-y^2}$ orbitals. Under D_2 symmetry the variation in the mixing parameter reflects essentially a variation in the S-Fe-S angles. Both interpretations are consistent with the idea that such angular variations are responsible for the two (at least) species observed in magnetic Mössbauer spectra of $[Fe(SCH_2CH_2OH)_4]^{2-}$. Thus, the observability of $S = 2$ EPR signals from $Fe(SR)_4$ sites appears to be highly sensitive to structural parameters whose variations have relatively low energy barriers. Indeed, the crystal structures of ferrous $Fe(SR)_4$ complexes show numerous S-Fe-S angles between 96 and 125°.[7,17,18] It is also noteworthy that the most angularly constraining ligand used in this study, namely, D,L-dihydrolipoate (which can form a six-membered S,S'-bidentate chelate ring vs seven-membered for dithiothreitol), forms the ferrous $Fe(SR)_4$ complex *not* exhibiting an $S = 2$ EPR signal. The fact that the ferrous $Fe(SR)_4$ complex of the tripeptide glutathione (γ-L-glutamyl-L-cysteinylglycine) shows an $S = 2$ EPR signal means that cysteine thiolate ligation permits observation of such a signal. The results presented here show that pseudotetrahedral high-spin ferrous complexes can give rise to $S = 2$ EPR signals. However, observability of such signals from biological $Fe(Cys\text{-}S)_4$ sites is likely to be strongly dependent on the protein matrix.[27]

Acknowledgment. This work was supported by National Institutes of Health Grants GM 40388 (D.M.K.) and GM32187 (B.H.H.) and by National Science Foundation Grant DMB8614290 (B.H.H.). D.M.K. (HL02207) and B.H.H. (DK01135) are NIH Research Career Development Awardees. We thank Elizabeth Holt for the X-ray diffraction results and Isabel Moura and Jean Le Gall for a sample of desulforedoxin.

Registry No. $[Fe(SCH_2CH_2OH)_4]^{2-}$, 119109-48-7; $Ba[Fe(SCH_2CH_2OH)_4]$, 119109-49-8; $[Fe(SCH_2CH_2OH)_4]^{-}$, 119109-50-1.

Supplementary Material Available: For $Ba[Fe(SCH_2CH_2OH)_4]$ tables listing atomic coordinates, bond distances and angles, and anisotropic thermal parameters (1 page); a table of F_o and F_c values (3 pages). Ordering information is given on any current masthead page.

(26) Bertrand, P.; Gayda, J.-P. *Biochim. Biophys. Acta* **1988**, *954*, 347-350.

(27) EPR signals with line shapes and g values nearly identical with those of Figures 1 and 2 have recently been observed in partially iron-loaded samples of metallothionen, a cysteine-rich, metal-scavenging protein.[28]

(28) Werth, M. T.; Johnson, M. K. *Biochemistry*, in press.

Contribution from the Department of Chemistry, The University, Newcastle upon Tyne NE1 7RU, U.K.

pH Dependence of Rate Constants for Reactions of Cytochrome *c* with Inorganic Redox Partners and Mechanistic Implications

P. L. Drake, R. T. Hartshorn, J. McGinnis, and A. G. Sykes*

Received July 13, 1988

Rate constants for the oxidation of horse cytochrome *c*(II) with $[Co(phen)_3]^{3+}$ and $[Co(terpy)_2]^{3+}$ decrease (~30%) on decreasing the pH from 8 to 5, giving a pK_a value of 6.7 (average). No corresponding decrease is observed with tuna cytochrome *c*(II) (which has His26 but no His33) or with His33 diethyl pyrocarbonate (DEPC) modified horse cytochrome *c*(II). *Candida krusei* cytochrome *c*(II) gives a pK_a of 6.9, which is likewise assigned to His33. No dependence on pH is observed with the negatively charged oxidants $[Fe(CN)_6]^{3-}$ and $[Co(dipic)_2]^{-}$ or surprisingly with $[Co(terpy)_2]^{2+}$, $[Ru(NH_3)_5py]^{2+}$, and $[Co(sep)]^{2+}$ as reductants for horse cytochrome *c*(III). Previous work using CDNP-modified horse cytochrome *c* derivatives has indicated that the positively charged redox partners $[Co(phen)_3]^{3+}$ (oxidant) and $[Co(sep)]^{2+}$ (reductant) react preferentially at site II on the front face of the molecule to the right-hand side of the solvent-accessible heme edge (the latter vertical with axially coordinated Met to the left), whereas negatively charged $[Fe(CN)_6]^{3-}$ reacts at site III to the left-hand side and across the top section of the exposed heme edge. His33 is close to site II, consistent with the effect of protonation of this residue on reactivity with the 3+ oxidants. Reduction potentials for horse cytochrome *c* determined electrochemically in the presence of a mediator show no variation with pH over the range 7.5-5. Protonation of His33, the imidazole ring of which is 12 Å from Fe, has no effect on the reduction potential therefore, and its effect on reactivity is a local effect. It is not immediately clear why there is no dependence on pH for the reaction of cytochrome *c*(III) with the three positively charged reductants. Possible contributing factors include some sort of conformational change, with a resultant shift in the site for electron transfer in the case of for example $[Co(terpy)_2]^{2+}$ as compared to $[Co(terpy)_2]^{3+}$, and effects stemming from different degrees of solvation at or near His33. His33 of horse cytochrome *c* gives virtually identical pK_a's and rates of DEPC modification for both the oxidized and reduced forms, indicating similar degrees of accessibility.

Introduction

Studies aimed at understanding the reactivity of cytochrome *c* (~104 amino acids; MW 12 400) with small inorganic redox partners are a subject of continuing interest.[1,2] Horse-heart cytochrome *c* is the main subject of the present study, where comparisons with tuna and *Candida krusei* cytochrome *c*'s have proved invaluable in assigning the histidine involvement.[3-6] Amino acid sequences for all three cytochrome *c*'s have been determined (and compared),[2] and X-ray structures of tuna[7] and rice[8] cyto-

(1) Moore, G. R.; Pettigrew, G. W. *Cytochromes c*; Springer-Verlag: New York, 1987.

(2) Moore, G. R.; Eley, C. G. S.; Williams, G. *Adv. Inorg. Bioinorg. Mech.* **1984**, *3*, 1-96.

(3) Margoliash, E.; Smith, E. L.; Kreil, G.; Tuppy, H. *Nature (London)* **1961**, *192*, 1125.

(4) Kreil, G. *Hoppe-Seyler's Z. Physiol. Chem.* **1963**, 334, 154; **1965**, *340*, 86.

(5) Narita, K.; Titani, K. *J. Biochem. (Tokyo)* **1968**, *63*, 226.

(6) Lederer, F. *Eur. J. Biochem.* **1972**, *31*, 144.

0020-1669/89/1328-1361$01.50/0